Journal of Engineering for Development

Journal of Engineering for Development, Vol. 13(1), October (2021) pp.64-75

POROSITY MODELING OF A NIGER DELTA FIELD UTILIZING THE SIMPLE KRIGING TECHNIQUE AND DETECTION OF ARTIFICIAL FEATURES IN GUASSIAN PROCESSES

[1]Mekunye, F. and [2]Ogbeide, P. O.

[2]Department of Petroleum Engineering, University of Benin, Benin City, Edo State, Nigeria
[I, 2] Email: mekunyefrancis@gmail.com, paulogbeide@yahoo.com

ABSTRACT

The main objectives of this study are analysis of spatial behavior of the porosity and presenting direction of anisotropy for the variable and describing variation of the parameter in a major reservoir in a Niger Delta field. Porosity well log data of 25 wells were available for performing this modeling. A univariate statistical analysis is done on the property to provide a framework for geostatistical analysis, modeling and data description purposes. The experimental semivariogram of porosity in different directions as well as the variogram map were plotted to find out the direction of anisotropy and the geostatistical parameters such as range, sill, and nugget effect for spatial analysis and subsequently for geostatistical modeling. Simple kriging with a constant and non-varying mean was used generate the porosity map of the reservoir. Analysis of the results indicates that the porosity values across the entire reservoir would approximate a normal distribution. Statistical analysis shows that the reservoir rock was a fairly porous sandstone. it can also be seen from the estimation variance map that the kriging error was uniformly low in regions where wells were concentrated and higher in other areas. Maximum direction of continuity was found to be N45W. The presence of artificial features was observed in kriged model and possible fixes were developed. Cross-validation can also be used to validate the generated model.

Keywords: Semivarogram; SGeMS; Geostatistical; Sill; Nugget; Kriging

Article Information:
Received 19 August, 2021
Revised 07 October, 2021
Accepted 10 October, 2021
Available online 08 March, 2022

1.0 Introduction

Porosity of reservoir rock is defined as the pore fraction of the rock—that is, the ratio of pore space volume to bulk volume of the rock. Porosity is usually expressed as a percentage and is one of the most important properties of the reservoir as it determines how much volume the rock can store under a given pressure system. Fluid-productive sandstones display porosities ranging between 0.05 and 0.4, or 5%–40%. Although the porosity of carbonate base material is practically zero, the overall porosity of carbonate rocks can be significant due to natural fractures within the rocks. It goes without saying that reservoir modeling is one of the most important tasks for geologists/reservoir engineers as it is the most useful problem-solving tool to the reservoir scientist. The accuracy of the dynamic simulation results is dependent on the accuracy and dependency on the initialization data of which the porosity model is a major part of. The reservoir void volumes are measured at low errors along control locations (location of wells) and also need to be accurately estimated at other unmeasured locations, and this is the function of spatial geostatistics.

Maps and mapmaking are integral parts of reservoir characterization. A map is a numerical model of an attribute's (e.g., porosity, permeability, thickness, structure) spatial distribution (Malvić and Jović 2012; Huysmans and Dassargues 2013). However, mapping an attribute is rarely the goal; rather, a map is used to make a prediction about the reservoir. To paraphrase Andre Journel of Stanford University, "A map is a poor model of reality if it does not depict characteristics of the real spatial distribution of those attributes that most affect how the reservoir responds".

The enormous up-front investments for developing heterogeneous fields and the desire to increase ultimate recovery have spurred oil companies to use innovative reservoir characterization techniques (Habibnia and Momeni 2012; Abdideh and Mahmoudi 2013). Geostatistics is one of many new technologies often incorporated into the process (Chen Y et al. 2011). For more than a decade, geostatistical techniques, especially when incorporating 3-D seismic data, have been an accepted technology to characterize petroleum reservoirs (Nava et al 2010; Kelsall and Wakefield 2002; Fegh et al. 2013).

However, unlike the deterministic approach, geostatistics provides numerous plausible results (Zarei et al. 2011). The degree to which the various models differ is a reflection of the unknown or a measurement of the "uncertainty". Some outcomes may challenge prevailing geologic wisdom and will almost certainly provide a range of economic scenarios, from optimistic to pessimistic. Having more than one result to analyze changes the paradigm of traditional reservoir analysis and may require multiple reservoir flow simulations (Soleymani and Riahi 2012). However, the benefits outweigh the additional time and cost.

This paper focuses on the use of the simple kriging technique to create an exhaustive 3D porosity model of a reservoir using well log porosity data. The major difference between both kriging methods is that simple Kriging assumes that the mean of the distribution is constant and stationary while ordinary kriging tries to predict the mean at every location together with the property to be estimated. Here, we would be making the assumption that the mean is constant and non-varying. Some limitations were encountered. The 3D cartesian grid applied

in this study may not be sufficient in describing the geometry of the actual reservoir which is more complex with irregular undulations and faults. Only porosity data was available for the static modeling workflow. More well data categories (thickness, permeability, kh etc.) would have given a more comprehensive geological study of the reservoir of interest. This study does not include the use of kriging with trends (KT), indicator kriging and kriging with a locally varying mean (LVM) together with indicator and conditional simulation which are other geostatistical tools that could produce desired results.

2.0 Mathematical Background

The simple kriging set of equations are derived from the expression of the estimation variance as stated below

$$E\{[R^*(x)]^2\} - 2E\{R^*(x)R(x)\} + E\{[R(x)]^2\} \quad (1)$$

Which when expanded leads to

$$\sum_{\alpha=1}^{n}\sum_{\beta=1}^{n}\lambda_\alpha\lambda_\beta \mathrm{E}\left[\mathrm{R}(\mathrm{x}_\alpha)\mathrm{R}(\mathrm{x}_\beta)\right] - 2\sum_{\alpha=1}^{n}\lambda_\alpha E[R(x)R(x_\alpha)] + E\left[\left(R(x)\right)^2\right] \quad (2)$$

Where,

$\sum_{\alpha=1}^{n}\sum_{\beta=1}^{n}\lambda_\alpha\lambda_\beta \mathrm{E}\left[\mathrm{R}(\mathrm{x}_\alpha)\mathrm{R}(\mathrm{x}_\beta)\right] = \sum_{\alpha}^{n}\sum_{\beta}^{n}\lambda_\alpha\lambda_\beta \mathrm{C}(x_\alpha, x_\beta)$ accounts for the data redundancy, covariance between sample data.

$\sum_{\alpha=1}^{n}\lambda_\alpha E[R(x)R(x_\alpha)] = \sum_{\alpha}^{n}\lambda_\alpha\, C(x, x_\alpha)$ - accounts for the closeness, covariance between unknown data point and sample data.

And since our aim is to optimize the weight to produce the minimum required error, we take a partial differential and set to zero.

$$\frac{\partial\varepsilon}{\partial\lambda} = \sum_{\beta=1}^{n}\lambda_\beta \mathrm{C}(x_\alpha, x_\beta) - 2\,\mathrm{C}(x, x_\alpha) \quad (3)$$

$$\sum_{\beta=1}^{n}\lambda_\beta \mathrm{C}(x_\alpha, x_\beta) = \mathrm{C}(x, x_\alpha) \quad (4)$$

3.0 Properties of Simple Kriging

1. The kriging estimator is unbiased
   $$E[Z(x) - Z^*(x)] = 0 \quad (5)$$
2. Minimum variance estimator
3. Third best Linear Unbiased estimator
4. Provides us an idea of our error
   $$Var_{\min}(x) = Var(Z) - \sum_{\alpha=1}^{n}\lambda_\alpha Cov_R(x_\alpha - x) - \mu \quad (6)$$
5. Exact interpolator: at data locations
6. Error term is homoscedastic, i.e the variance of the errors should not change between difference observations

3.0.1 Artificial features in kriging

Generally, global kriging may not be desired because the mean is not constant over the domain and also may be not plausible when you have a lot of data which means we would have to invert a large covariance matrix. Therefore, it would be necessary to perform a" local" kriging using a limited search neighborhood, which would be a user defined search ellipsoid (which may lead to artifacts). Artificial features as observed above in the local kriging result are not entirely desirable. They occur when a small shift Δx from a previously estimated observed point discounts a significantly large $Z(x_\alpha)$ which was present in the defined neighborhood of the previously estimated data point (Isaaks EH et al., 1989).

4.0 Methodology

4.0.1 Data Description

The geostatistical approximation approach for reservoir modeling is presented in this work. Data on reservoir flow units for porosity was obtained from 25 wells for this study. The distance between wells is rather uneven, and the property appears to be distributed normally. The porosity was calculated using sonic and neutron logs. The data that was imported into the SGeMS environment containing 2500 data points with positions scattered around space and concentrated in regions with more wells as can be expected.

The data was visually examined after being imported into the SGeMS environment as an object called "rock void fraction." It was then essential to figure out how the property was distributed over the reservoir. As shown in Figure 1 and 2, a probability distribution function and a probability density function were created. The resulting histogram revealed that the property was about normally distributed**.**

A mean of 0.282359 was observed together with a variance of 0.00780609.

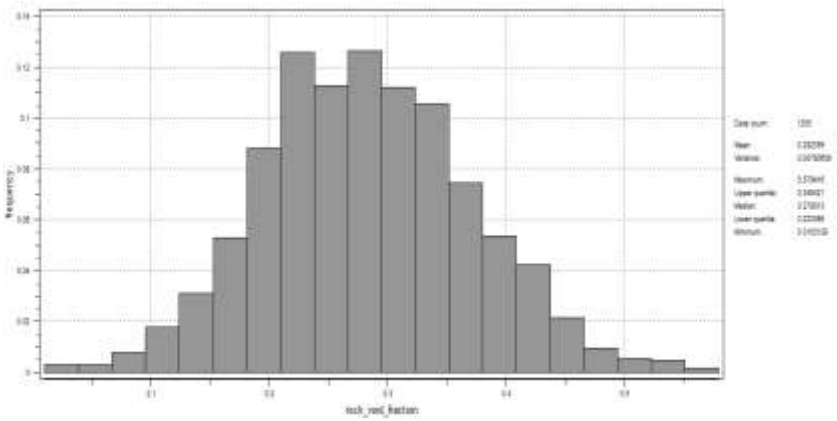

Figure 1: Probability density function of porosity

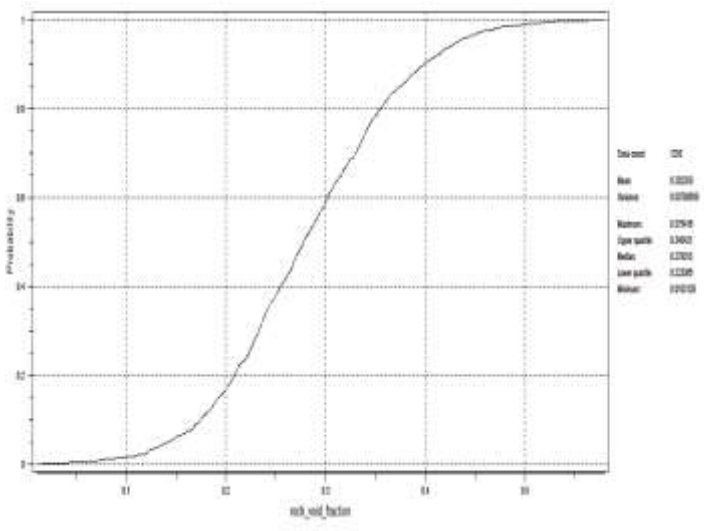

Figure 2: Cumulative distribution function of porosity

4.0.2 Variography (spatial structural analysis)

Kriging solves a linear system of equations and the system has to remain positive definite and should not be singular. Can any random interpolation method be applied? No. Why? Our estimation variance given as:

$$Var_{\min}(x) = Var(Z) - \sum_{\alpha=1}^{n} \lambda_\alpha Cov_R(x_\alpha - x) - \mu \quad (7)$$

and so, the estimation variance has to remain positive for it to be meaningful, and so we need to have functions that we know prior, and that has been investigated that would always provide us with positive results. In order to do kriging, we need to understand the variability of our data for a particular lag distance and this forms an important reason to create an accurate variogram model of our data. Only distance for which the variogram is calculated are distances between data locations, and not distances between data and locations to be estimated. The usual estimator of the variogram function for lag distance h (that is, for those pairs separated by a vector, $\vec{h}$) is;

$$\gamma(h) = \frac{1}{2N_h} \sum_{i,k\varepsilon P_h}^{N_h} (z_i - z_{j)}{}^2 \quad (8)$$

where N_h is the number of distinct pairs of data values, placed in the set P_h (pairs displaced by the vector $\vec{h}$. It can be shown that the sample variogram obtained using this estimator can be considered a spatial decomposition of the sample variance

The variogram modeling procedure was initiated taking the porosity as both head and tail property. 27 lags were utilized with a unit lag distance and lag tolerance. The semivariance was generated for 7 directions which includes azimuth=0: dip=45, azimuth=90: dip=45, azimuth=45: dip=45, azimuth=90: dip=90, azimuth=35: dip=65, azimuth=45: dip=0, azimuth=0: dip=0. The second direction with equal azimuth and dip was taken as the omni-directional variogram with a tolerance of 180 and a bandwith of 25. The plots were generated and the nugget effect was intelligently selected and a model was fitted into the experimental

variogram by changing the maximum, medium and minimum range values together with the sill until a reasonable fit was gotten.

Table 1: variogram directions

Azimuth	Dip	Tolerance	Bandwidth	Measure type	Calculation base
0	**45**	**22.5**	**15**	**Semi-variance**	**H-T**
90	**45**	**22.5**	**25**	**Semi-variance**	**H-T**
45	**45**	**22.5**	**26**	**Semi-variance**	**H-T**
90	**90**	**22.5**	**18**	**Semi-variance**	**H-T**
35	**65**	**22.5**	**15**	**Semi-variance**	**H-T**
45	**0**	**22.5**	**33**	**Semi-variance**	**H-T**
45	**30**	**180**	**30**	**Semi-variance**	**H-T**

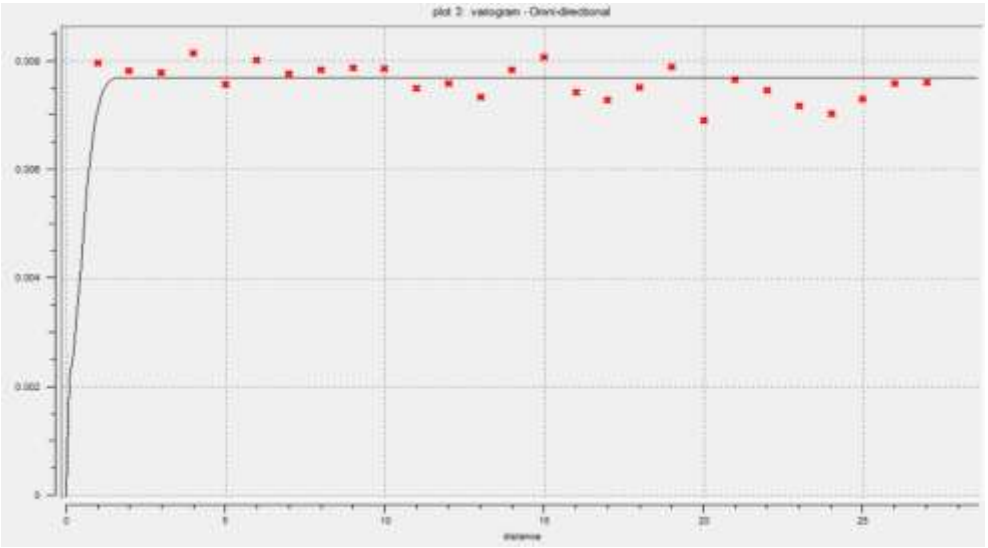

Figure 3: Model fitted to semi-variance, omni direction

The sill was estimated to be 0.0057 with a nugget effect of 0.002. The maximum, medium and minimum ranges that fitted the model were 8.91, 4.05 and 0.81 respectively. The resulting variogram was a single structure.

4.0.3 Simple Kriging

Kriging was performed using the "kriging blocks and points" algorithm in SGeMS. Initially a Cartesian grid was created that could completely fill the data region in the 3D space. The Cartesian grid had dimensions of 200*200*50 with 2,000,000 grid cells. The grid dimension was chosen by checking the maximum values in all directions and this grid would represent the reservoir formation in this study. The variogram model was imported into the kriging environment of SGeMS where the simple Kriging algorithm was implemented. The mean (0.23) of the distribution was assumed to be known and constant at every point and SK was performed. The maximum and minimum conditioning data were 50 and 100 respectively. The contribution was set as contribution=sill-nugget with a single structure. The geometry and orientation of the search ellipsoid was defined with a maximum range of 80, medium range of 40 and minimum range of 10. The azimuth was set at 45 with a dip of 45 and rake angle of 10. The variogram type was observed to be gaussian in nature. The SK algorithm was ran.

5.0 Results and Discussion

The simple kriging 3D map showed that the central region of the reservoir showed a slightly greater void fraction and the high porosity phenomenon is seen to be spatially continuous over the region. The result is quite neat and smooth as expected from kriging, as it is an exact interpolator in sampled locations and tries to smoothen the variation of the known property around unsampled regions. This region of high porosity could be as a result of the presence of high quality sand with similarly high permeability values.

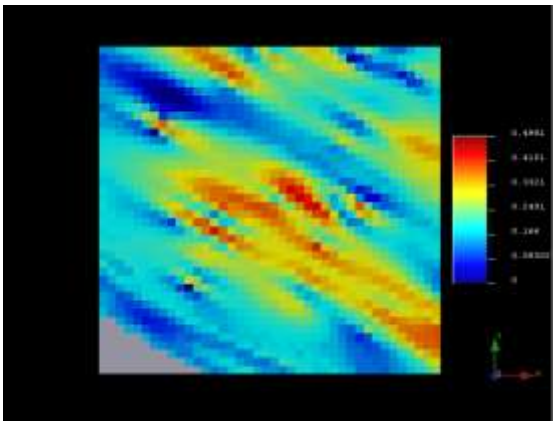

Figure 4: SK XY map

It can also be observed that the kriging algorithm has respected the presence of spatial continuity and it can be seen in the XY map above as regions of similar property value seem to continue laterally over the given space. The distribution of the result was analyzed and it was found that the property is approximately normally distributed as can be seen in Figure 5 with a mean of 0.243493 and a variance of 0.00626. The upper quantile was 0.295584 and the lower quantile was 0.189246. The maximum was 0.489132 and a minimum of 0.023440. it can also be seen from the estimation variance map that the kriging error was uniformly low in regions where wells were concentrated and higher in other areas.

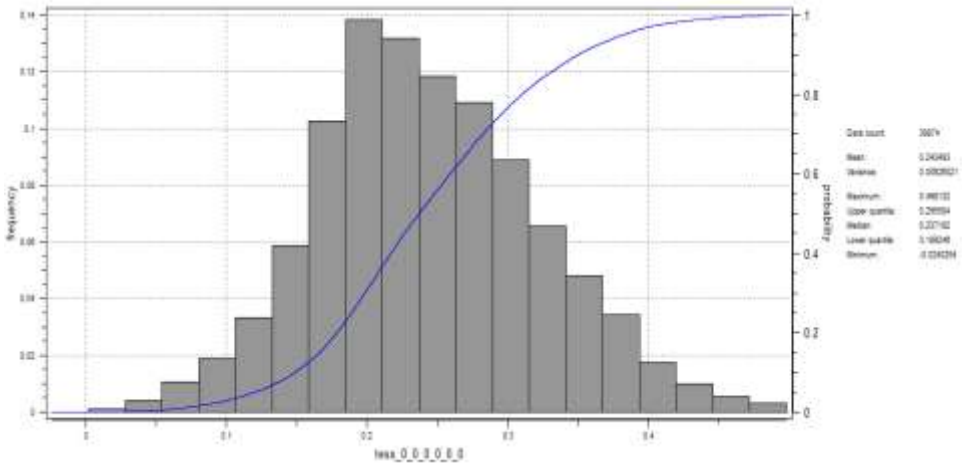

Figure 5: PDF and CDF of SK generated result

The P-P (percentile-percentile) and Q-Q (quantile-quantile) plot was generated in the SGeMS environment and it was analyzed. The plots were generated with 2 variables, variable 1 was the initial sample data and variable 2 was the generated kriging values. The resulting plots as seen below indicates that the estimation distribution and the original data set can be said to be from the same distribution because it almost fits into a straight line.

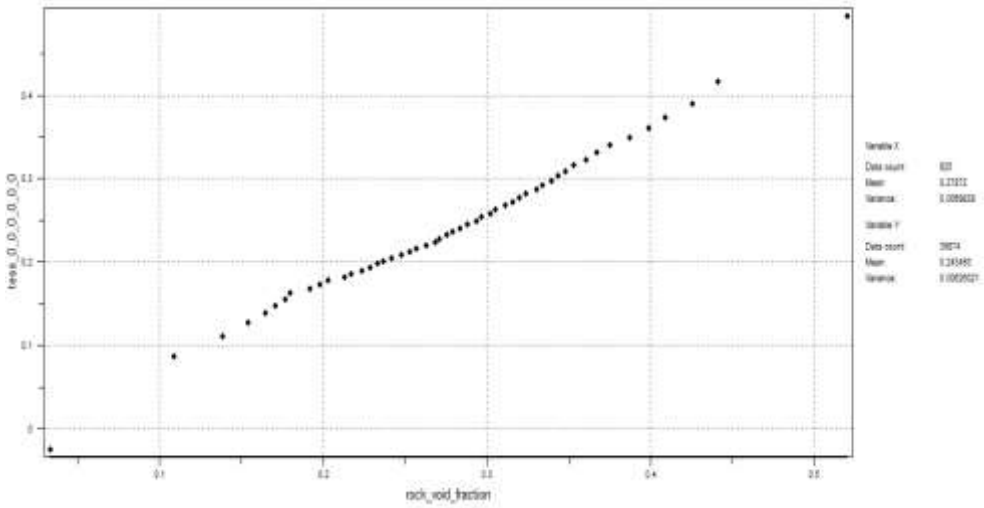

Figure 6: Q-Q plot of SK results and sample data

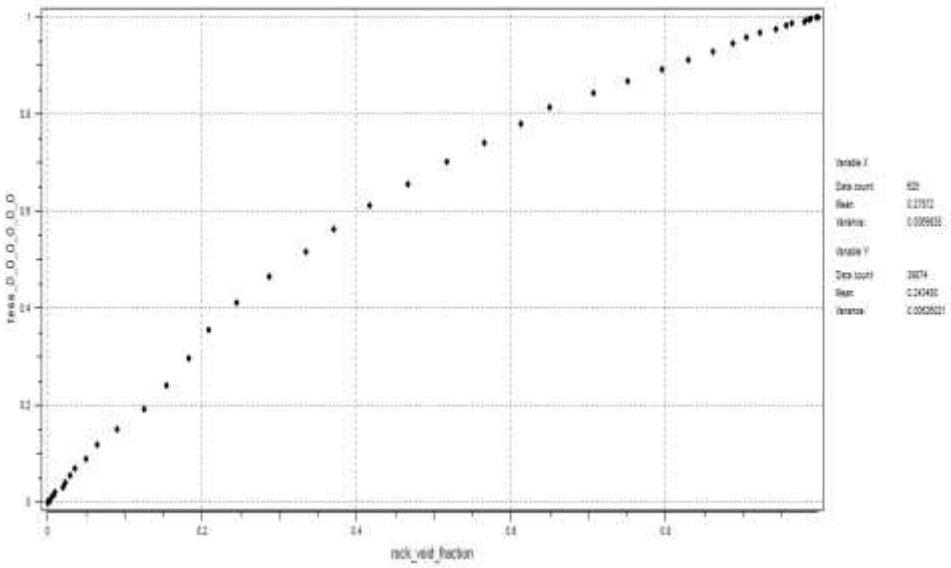

Figure 7: P-P Plot of SK results and sample

5.1 Presence of Artifacts

The SK algorithm was ran for the second time with a change in the orientation of the search ellipsoid (maximum range of 100, medium range of 50 and minimum range of 15). The results were exactly the same as observed early only with a slight difference which is observed in the ZY plane.

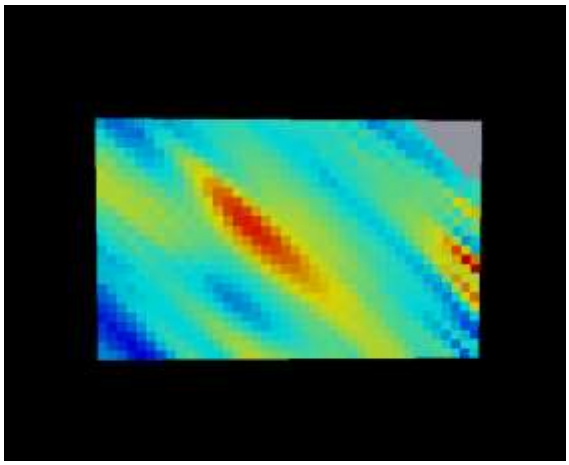

Figure 8: ZY Plane porosity map at modified search ellipsoid

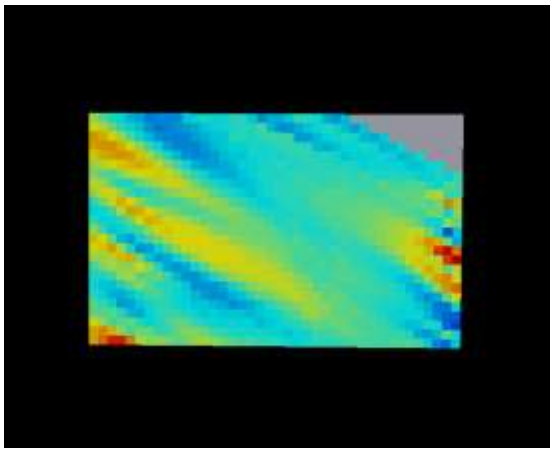

Figure 9: ZY Plane porosity map at normal search ellipsoid

It can be seen that a high porosity phenomenon observed in our normal search ellipsoid vanishes when the dimensions of the search neighborhood is enlarged. This is called an artificial feature and can lead to very misleading stochastic maps. Artifacts are very common with kriging (simple or ordinary) as the estimation results are very dependent on the spatial orientation of conditioning constraints. Artifacts are caused when a significant outlier data (extremely high or small) becomes included or excluded from the conditioning data when the dimensions of the ellipsoid in space is altered even slightly.

5.2 Possible fixes for implementation

Instead of using a search neighborhood, we could define a minimum amount of points in your search neighborhood. That would try to mitigate the problem of a shifting neighborhood. In this method, your effective search radius is dependent on where you are, so we would have different effective search radius at different locations because you are using different amount of data in that search neighborhood and also because of the configuration of your data, sometimes your search radius might contain extreme values.

Another fix is to add a penalty to the diagonal of the system of equations, that we you are trying to decrease the influence of data that are further apart and decrease the influence of the covariance of the diagonal such that:

$$penalty = \sum_{\alpha=1}^{n} {\lambda_\alpha}^2 \varepsilon(x_\alpha) \Rightarrow$$
$$\begin{cases} \sum_{\beta=1}^{n} \lambda_\beta Cov_R(x_\alpha - x_\beta) + \mu + \sum_{\alpha=1}^{n} \lambda_\alpha \varepsilon(x_\alpha) = Cov_R(x - x_\alpha) \\ \sum_{\beta=1}^{n} \lambda_\beta = 1 \end{cases} \quad (9)$$

6.0 Conclusions

This paper have used a geostatistical technique, simple kriging, to model porosity data in a filed in the Niger Delta region. The porosity range in the area is 0.05-0.48, which suggests that the lithology could be sand or shale. The simple kriging 3D map showed that the central region of the reservoir showed a slightly greater void fraction and the high porosity phenomenon is seen to be spatially continuous over the region across from the north eastern to south western region of the reservoir. The standard deviation for the entire field ranges from 0.04–0.08. Based on this, linear and parametric geostatistics were employed to process the data in order to build

geostatistical model of the subsurface geology. The semivariogram shows the major direction of continuity “azimuth of 45”, spherical geometrical anisotropy. Simple Kriging map shows clearly vertical and horizontal heterogeneity of the study area and subsurface interbedded layers, which agrees with the result of the semivariogram. As part of the assumptions of the technique a constant and stationary mean was used to krig. The Kriging technique can be seen to have uncalculated regions as observed in the south western region of the XY map (and as can be seen in the 3D map) as kriging could not performed in those regions because of nature of data and this is a major drawback. The technique was sensitive to the geometry and orientation of the search neighborhood and it required several attempts (about 22) to produce desired results which was time consuming. Artificial features were observed in the kriging results as we attempt to slightly change the search neighborhood and this can lead to very misleading results. Although artifacts are quite technical and difficult to eliminate, possible fixes were introduced with the inclusion of a penalty to the system of equations.

7.0 Recommendation

The simple kriging map can be accurate but is not best possible. Cross validation of model can be performed with ordinary kriging, kriging with trends and kriging with a locally varying mean whose techniques are more robust and tend to reduce estimation error with fewer assumptions in their system of equations. Lastly, all possible kriging estimations can be improved and compared by performing simulation on the required sample data after kriging as simulation is known to produce the most desirable results in the industry.

REFERENCES

Abdideh M, Mahmoudi N (2013) UCS prediction: a new set of concepts for Reservoir Geomechanical Modeling. Pet Sci Technol 31(24):2629–2635.

Chen Y, Park K, Durlofsky L (2011) Statistical assignment of upscaled flow functions for an ensemble of geological models. Comput Geosci 15(1):35–51.

Fegh A, Riahi M, Norouzi G (2013) Permeability prediction and construction of 3D geological model: application of neural networks and stochastic approaches in an Iranian gas reservoir. Neural Comput & Applic 23(6):1763–1770.

Habibnia B, Momeni A (2012) Reservoir characterization in Balal oil field by means of inversion, attribute, and geostatistical analysis methods. Pet Sci Technol 30(15):1609–1618.

Huysmans M, Dassargues A., (2013) The effect of heterogeneity of diffusion parameters on chloride transport in low-permeability argillites. Environ Earth Sci 68(7):1835–1848.

Kelsall J, Wakefield J (2002) Modeling spatial variation in disease risk. JAm Stat Assoc 97(459):692–701.

Malvić T, Jović G (2012) Thickness maps of neogene and quaternary sediments in the Kloštar Field (Sava Depression, Croatia). J Maps 8(3):260–266.

Nava E, Pintos S, Queipo NV (2010) A geostatistical perspective for the surrogate-based integration of variable fidelity models. J Pet Sci Eng 71(1–2):56–66.

Soleymani H, Riahi MA (2012) Velocity based pore pressure prediction—A case study at one of the Iranian southwest oil fields. J Pet Sci Eng 94–95:40–46.

Zarei A, Masihi M, Salahshoor K (2011) Comparison of different univariate and multivariate geostatistical methods by porosity modeling of an Iranian oil field. Pet Sci Technol 29(19):2061–2076.

APPENDICES

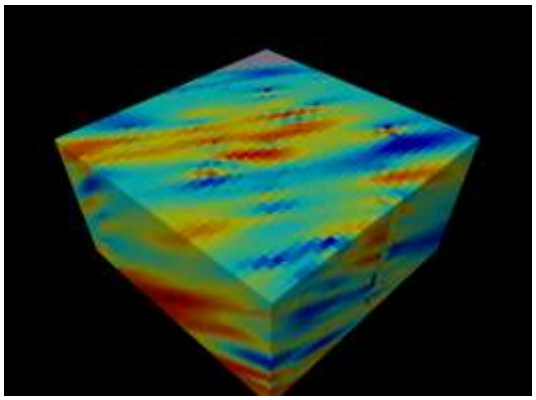

Figure 10: 3D model, SK

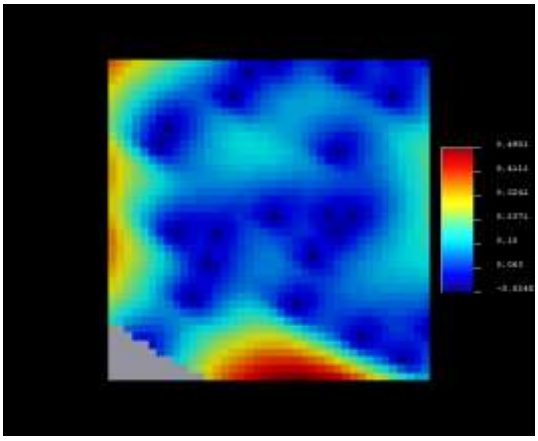

Figure 11: Estimation variance distribution